13

On the Optical Response of Nanoparticles: Directionality Effects and Optical Forces

Braulio García-Cámara[1], Francisco González[1], Fernando Moreno[1], Raquel Gómez-Medina[2], Juan José Sáenz[2] and Manuel Nieto-Vesperinas[3]
[1]*Grupo de Óptica, Departamento de Física Aplicada, Universidad de Cantabria*
[2]*Departamento de Física de la Materia Condensada, Universidad Autónoma de Madrid*
[3]*Instituto de Ciencias de los Materiales de Madrid, CSIC*
Spain

1. Introduction

Nowadays, miniaturization is a general challenge for technology. Researchers in science and technology claim to study ever smaller systems and develop ever smaller devices. The nanometric range is, at present, an important focus of attention of scientists and engineers following the famous prediction by Prof. Feynman: "There's plenty of room at the bottom". Reduction of dimensions, at this level, involves that more specific and more complex tools are needed.

Light has appeared as a convenient solution for these tasks because of its wavelength (hundreds of nanometers) and the large amount of information it contains about systems with which it interacts (Prasad, 2004). The interaction of light with small systems, either particles or structures, gives rise to several scattering phenomena which are strongly dependent on both the characteristics of the incident radiation (frequency, polarization) and those of the object (size, shape, optical properties). These interactions can be used either to obtain information about the interacting object (e.g. particle sizing) (Zhu et al., 2010) or to produce light scattering phenomena "à la carte" by means of suitable nanoobjects.

At the nanoscopic level, the interaction between an incident beam and a metallic system produces an interesting physical phenomenon which is the base of many technological applications in diverse fields like medicine, biology, communications, information storing, energy transformation, photonics, etc (Anker et al., 2008; Maier et al., 2003). This is the excitation of *localized surface plasmon resonances* (*LSPR*) (Prasad, 2004). For these, the electromagnetic field experiences a high localization in the scatterer and a strong enhancement out of the scatterer.

These advances have stimulated new research devoted to obtain a greater control over how light is scattered by these systems. Researchers have analyzed emerging structures (nanoholes (Gao et al., 2010), nanocups (Mirin & Halas, 2009), etc). But, what it is more interesting, new engineered materials, called *metamaterials* and whose optical properties can be manipulated, have been developed (Boltasseva & Atwater, 2011). The possibility to obtain structures with

optical properties "à la carte" allows getting scattering phenomena never observed before in natural media, for instance negative refraction (Shalaev, 2008). The main consequences of negative refraction are the two interesting potential applications: cloacking (Pendry et al., 2006) and perfect lens (Pendry, 2000; Nieto-Vesperinas & Garcia, 2003).

The control over the values of both the electric permittivity and the magnetic permeability of an object gives us a control over the way it scatters light, and in particular, the angular distribution of the scattered radiation. This control could involve a dramatic evolution on the field of nanodevices. For this reason, the objective of this chapter is to analyze directional effects on both light scattering and optical forces of a nanoparticle with convenient optical constants. The structure of the chapter is as follows: while sections 2, 3 and 4 are devoted to the directional features on light scattering by nanoparticles, section 5 summarizes the main results on optical forces. Finally, the most important conclusions about these results are recapitulated in section 6.

2. Light scattering by nanoparticles

2.1 Mie theory

The problem of the electromagnetic scattering from an isolated and spherical particle was firstly solved in 1908 by Gustav Mie (Mie, 1908). However, this simple system still involves interesting physical behaviors that are worthy of further study.

Mie theory considers a spherical particle of radius a and optical constants given by an electric permittivity, ε_p, and a magnetic permeability, μ_p, immersed in a homogeneous and isotropic medium. This is illuminated by a linear polarized plane wave, as in Figure 1. Without loss of generality, we assume that the surrounding medium is vacuum ($\varepsilon_s=\mu_s=1$). The scattered electromagnetic field ($\mathbf{E}_s$, $\mathbf{H}_s$) can be expressed as a multipole expansion of *Vector Spherical Harmonics (VSH),* called Mie expansion, as follows

$$\mathbf{E}_s = \sum_{n=1}^{\infty} E_n \left(i a_n \mathbf{N}_{e\ln}^{(3)} - b_n \mathbf{M}_{o\ln}^{(3)} \right) \tag{1}$$

$$\mathbf{H}_s = \frac{k}{\omega \mu_p} \sum_{n=1}^{\infty} E_n \left(i b_n \mathbf{N}_{o\ln}^{(3)} + a_n \mathbf{M}_{e\ln}^{(3)} \right) \tag{2}$$

where $k = m\omega / c = m2\pi / \lambda$, λ being the incident wavelength in vacuum, $m = \sqrt{\varepsilon_p \mu_p}$ the refractive index of the particle, c the speed of light in vacuum and ω the angular frequency of the incident wave. E_n is defined as $E_n = E_0 i^n \frac{2n+1}{n(n+1)}$, E_0 being the amplitude of the incident plane wave. The series are characterized by the a_n and b_n Mie coefficients which are defined as (Bohren & Huffman, 1983)

$$a_n = \frac{\mu_s m^2 j_n(mx)\left[x j_n(x)\right]' - \mu_p j_n(x)\left[mx j_n(mx)\right]'}{\mu_s m^2 j_n(mx)\left[x h_n^{(1)}(x)\right]' - \mu_p h_n^{(1)}(x)\left[mx j_n(mx)\right]'} \tag{3}$$

$$b_n = \frac{\mu_p m^2 j_n(mx)\left[xj_n(x)\right]' - \mu_s j_n(x)\left[mxj_n(mx)\right]'}{\mu_p m^2 j_n(mx)\left[xh_n^{(1)}(x)\right]' - \mu_s h_n^{(1)}(x)\left[mxj_n(mx)\right]'} \tag{4}$$

x being the size parameter, that is defined as

$$x = ka = \frac{2\pi a}{\lambda}, \tag{5}$$

In addition, j_n are the *spherical Bessel functions* and $h_n^{(1)}$ the *spherical Bessel functions of third kind* or *Hankel functions*. As the electric and magnetic dipolar contributions are weighted by coefficients a_1 and b_1, respectively, the quadrupolar ones by a_2 and b_2 and so on, Mie coefficients a_n are associated to the electric part of the scattered electromagnetic radiation, while b_n are associated to the magnetic one.

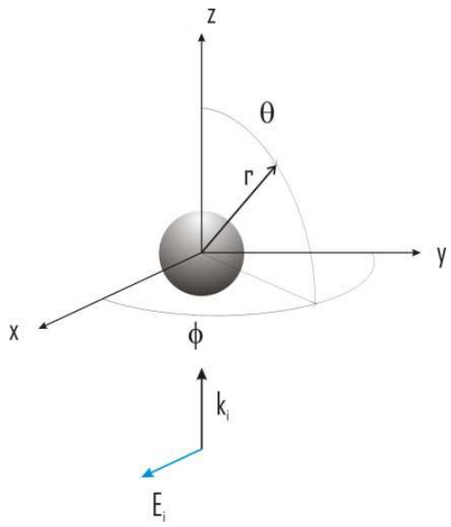

Fig. 1. Scheme of the geometry of the problem.

These coefficients contain the relevant information about essential scattering parameters as the extinction, C_{ext}, and scattering, C_{sca}, cross sections. These can be written as

$$C_{sca} = \frac{2\pi}{k^2}\sum_{n=1}^{\infty}(2n+1)(|a_n|^2 + |b_n|^2) \tag{6}$$

$$C_{ext} = \frac{2\pi}{k^2}\sum_{n=1}^{\infty}(2n+1)\mathrm{Re}(a_n + b_n) \tag{7}$$

2.2 Details of Mie theory at the nanoscopic level

If particle size is very small compared with the incident wavelength, that is $a/\lambda<<1$, dipolar contributions ($n=1$ in Eqs. (1)- (2)) clearly dominate and Mie coefficients of order higher than 1 can be neglected. Thus, the Mie expansion can be simplified and the previous parameters have simple expressions

$$C_{sca} = \frac{2\pi}{k^2}[3(|a_1|^2 + |b_1|^2)] \tag{8}$$

$$C_{ext} = \frac{2\pi}{k^2}[3\mathrm{Re}(a_1 + b_1)] \tag{9}$$

This is the case of a nanoparticle ($a < 50\ nm$) when it is illuminated by an incident wave in the visible or near infrared (NIR) part of the spectrum ($\lambda > 500\ nm$).

The predominant dipolar conduct, either electric or magnetic, of nanoparticles is usually described by the electric and/or magnetic complex polarizabilities, α_e and α_m, respectively. Both can also be expressed as a function of the two first Mie coefficients

$$\alpha_e = \frac{\alpha_e^{(0)}}{1 - i\frac{2}{3}k^3\alpha_e^{(0)}} = \frac{3i}{2k^3}a_1 \tag{10}$$

$$\alpha_m = \frac{\alpha_m^{(0)}}{1 - i\frac{2}{3}k^3\alpha_m^{(0)}} = \frac{3i}{2k^3}b_1 \tag{11}$$

where

$$\alpha_e^{(0)} = 4\pi a^3 \frac{\varepsilon_p - 1}{\varepsilon_p + 2} \tag{12}$$

$$\alpha_m^{(0)} = 4\pi a^3 \frac{\mu_p - 1}{\mu_p + 2} \tag{13}$$

are the static polarizabilities, defined in the limit $ka \rightarrow 0$.

3. Directional effects on light scattering by nanoparticles with arbitrary values of ε and μ.

3.1 Kerker's theory

In the early eighties, M. Kerker and co-authors (Kerker et al., 1983) presented an interesting study about the scattering properties, in the far field, of a spherical particle much smaller than the incident wavelength, illuminated by a plane wave and without any restriction for the values of its relative optical constants (ε and μ). Some interesting electromagnetic scattering effects were described in this work such as the zero-backward and the zero-forward scattering. Although the idea of a magnetic permeability different from 1 in the visible range was hypothetical and the described effects were thought to be impossible to be observed when the work was presented, the engineered metamaterials have currently revitalized these electromagnetic studies (Zhedulev, 2010).

In this section, the main theoretical aspects described by M. Kerker et al. are briefly reviewed.

3.1.1 Zero-backward scattering: First Kerker's condition

When we consider a system, like that of Figure 1, the scattered intensity in the scattering plane can be described by means of two polarized components: I_{TE} and I_{TM}. While I_{TE} corresponds to an incident electric field parallel to the scattering plane, I_{TM} corresponds to a perpendicular one. These components can be written as (Bohren & Huffman, 1983)

$$I_{TE} = \frac{\lambda^2}{4\pi r^2}\left|\sum_n \frac{2n+1}{n(n+1)}(a_n\pi_n + b_n\tau_n)\right|^2 \tag{14}$$

$$I_{TM} = \frac{\lambda^2}{4\pi r^2}\left|\sum_n \frac{2n+1}{n(n+1)}(a_n\tau_n + b_n\pi_n)\right|^2 \tag{15}$$

where r is the distance from the particle to the observer ($2\pi r/\lambda >> 1$) and π_n and τ_n are angular functions defined in (Bohren & Huffman, 1983). As we are considering a very small or dipole-like particle ($a \rightarrow 0$), only the two first Mie coefficients (a_1 and b_1) are introduced in the expressions. In addition some approximations can be applied to these coefficients in such a way that the scattered intensity components can be approximated by

$$I_{TE} = \frac{\lambda^2 x^6}{4\pi r^2}\left|\left(a_1 + b_1\cos\theta\right)\right|^2 = \frac{\lambda^2 x^6}{4\pi r^2}\left|\left(\left(\frac{\varepsilon-1}{\varepsilon+2}\right)+\left(\frac{\mu-1}{\mu+2}\right)\cos\theta\right)\right|^2 \tag{16}$$

$$I_{TM} = \frac{\lambda^2 x^6}{4\pi r^2}\left|\left(a_1\cos\theta + b_1\right)\right|^2 = \frac{\lambda^2 x^6}{4\pi r^2}\left|\left(\left(\frac{\varepsilon-1}{\varepsilon+2}\right)\cos\theta+\left(\frac{\mu-1}{\mu+2}\right)\right)\right|^2 \tag{17}$$

θ being the scattering angle, defined as the angle between the incident and the scattered directions (see Figure 1).

For the backward scattering direction ($\theta = 180^o$) the previous expressions adopt the following forms

$$I_{TE}(180^\circ) = \frac{\lambda^2}{4\pi r^2}x^6\left|\left(\left(\frac{\varepsilon-1}{\varepsilon+2}\right)-\left(\frac{\mu-1}{\mu+2}\right)\right)\right|^2 \tag{18}$$

$$I_{TM}(180^\circ) = \frac{\lambda^2}{4\pi r^2}x^6\left|\left(-\left(\frac{\varepsilon-1}{\varepsilon+2}\right)+\left(\frac{\mu-1}{\mu+2}\right)\right)\right|^2 \tag{19}$$

It easy to observe that when $\varepsilon = \mu$, or equivalently when $\alpha_e = \alpha_m$, the scattered intensity in the backward direction is zero for both incident polarizations. This is the *zero-backward scattering condition* and we shall call in the following the *first Kerker's condition*. In Figure 2 the

scattering pattern of a dipole-like particle with relative optical properties, $\varepsilon = \mu = 3$ is shown. Only a TM polarization is considered because, from Eqs. (18) and (19), the scattered intensity is equal for both polarizations under this condition.

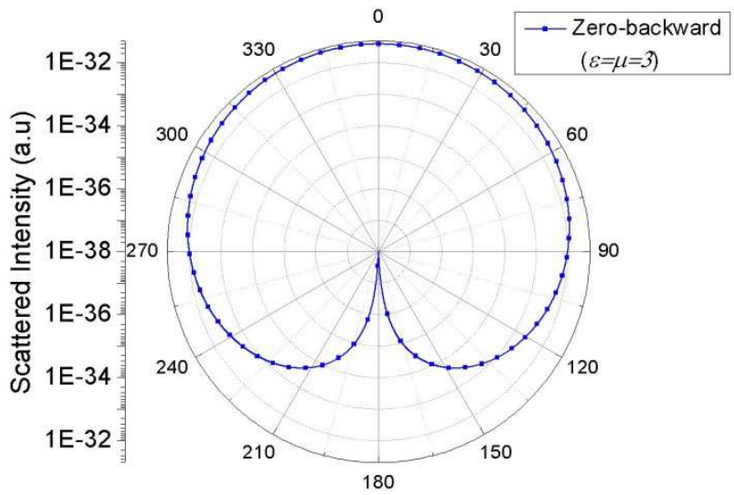

Fig. 2. Scattering diagram of a dipole-like particle ($a = 10^{-6}\lambda$) with relative optical properties fulfilling the zero-backward condition and for a TM incident polarization

3.1.2 Zero-forward scattering: Second Kerker's condition

For $\theta = 0^o$ (forward scattering direction), Eqs. (16)-(17) become

$$I_{TE}(0^\circ) = \frac{\lambda^2}{4\pi r^2} x^6 \left| \left(\left(\frac{\varepsilon - 1}{\varepsilon + 2}\right) + \left(\frac{\mu - 1}{\mu + 2}\right) \right) \right|^2 \tag{20}$$

$$I_{TM}(0^\circ) = \frac{\lambda^2}{4\pi r^2} x^6 \left| \left(\left(\frac{\varepsilon - 1}{\varepsilon + 2}\right) + \left(\frac{\mu - 1}{\mu + 2}\right) \right) \right|^2 \tag{21}$$

In this case, the ε–μ relation which cancel $I_{TE}(0^o)$ and $I_{TM}(0^o)$ is not as evident as before. However, Kerker et al. (Kerker et al., 1983) demonstrated that this happens when

$$\varepsilon = \frac{4 - \mu}{2\mu + 1} \tag{22}$$

which is equivalent to $\boldsymbol{Re(\alpha_e) = -Re(\alpha_e)}$ and $\boldsymbol{Im(\alpha_e) = Im(\alpha_e)}$. This is the *zero-forward scattering condition*, that we shall call the *second Kerker's condition*.

It is interesting to highlight that this condition is symmetric. This means that it remains invariant by interchanging ε and μ. An example of the angular distribution of the scattered intensity of a very-small particle satisfying this condition is shown in Figure 3 for a TM polarized incident beam (TE polarization produces a similar result).

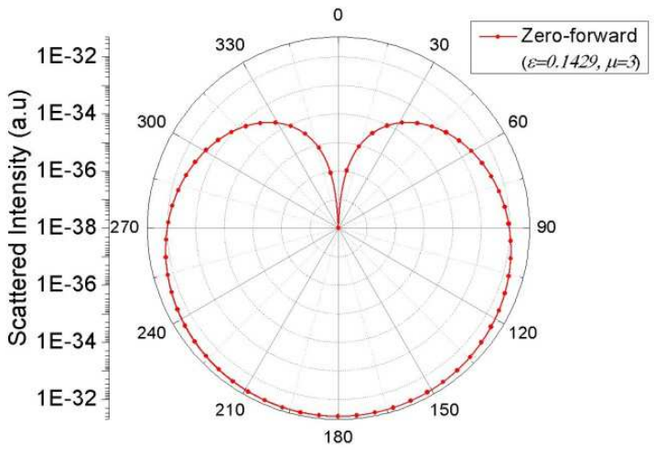

Fig. 3. Scattering diagram of a dipole-like particle ($a = 10^{-6}\lambda$) with relative optical properties fulfilling the zero-forward condition, ($\varepsilon; \mu$) = (0.1429; 3), and TM incident polarization.

3.2 An analysis of Kerker's conditions

Kerker's theory was developed under the far-field approximation and for the very particular case of dipole-like particles for which only the two first Mie coefficients (a_1 and b_1) are non negligible. However, as particle size increases or the observer approaches, other multipolar terms become important and the directional features, described previously, can be modified.

3.2.1 Size effects on the directionality conditions

One of the responsibles for the appearance of multipolar contributions is the size of the particle, a. When this deviates from the condition $a/\lambda<<1$, orders in the Mie expansion greater than *1* start to be non negligible. The purpose of this section is to analyze size effects on the two Kerker's conditions (García-Cámara et al., 2010a).

Zero-backward scattering condition can be extended even for large particle sizes. This is possible because the ε–μ symmetry of Mie coefficients (Eqs. (3)-(4)) ensures that all the electric and magnetic multipolar contributions are equal and with opposite sign at backward direction. This produces a destructive interferential effect between both contributions for every multipolar order and for a given particle size, a. Figure 4 shows the scattering diagrams for several particles with different size (a) and optical properties satisfying the zero-backward scattering condition ($\varepsilon=\mu$).

On the contrary, the zero-forward scattering condition is much more sensitive to size effects. In fact, as a increases and multipolar terms, other than the dipolar ones, become important, the electric and magnetic contributions in the forward direction do not interfere destructively anymore, and the zero-forward-scattering tends to disappear. In spite of this, it is possible to find pairs ($\varepsilon; \mu$) which minimizes the scattered intensity in the forward direction. In Figure 5, the distribution of the scattered intensity for spherical particles of different sizes is plotted. The values of ε and μ, which are included in the figure caption, were chosen such that a minimum of the scattered intensity in the forward direction

appears. For the smallest value of a, the scattered intensity in the forward direction is considerably lower compared to other angles. However, as a increases, this minimum becomes less pronounced due to the influence of quadrupolar terms.

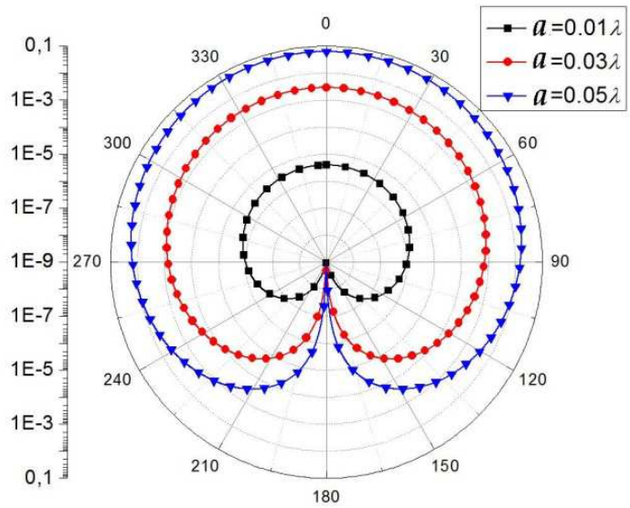

Fig. 4. Scattering diagrams, in logarithmic scale, for a spherical particle with relative optical properties (ε; μ) = (-3;-3) and illuminated by a TE-polarized incident light.
Several particlesizes have been considered.

In a recent research (García-Cámara et al., 2010a), it was found that these optical constants which minimize forward scattering don't follow Kerker's conditions but can be fitted to a formally similar expression where fitting coefficients are dependent on particle size.

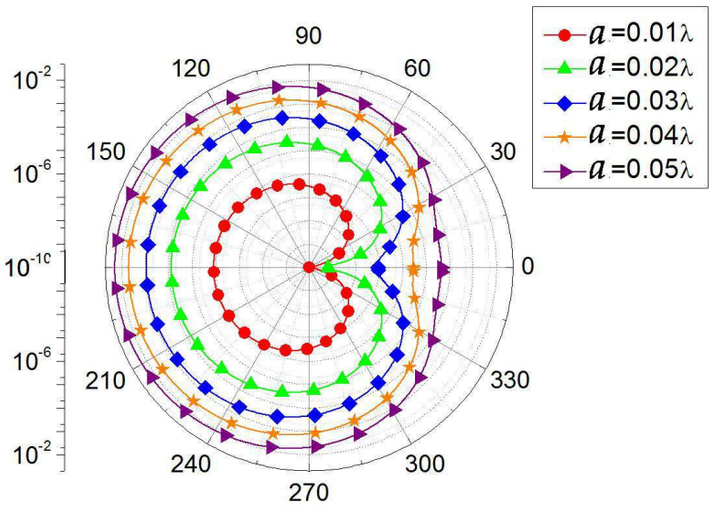

Fig. 5. Scattering diagrams, in logarithmic scale, for a spherical particle illuminated with a TE linearly polarized incident beam. For each particle size, optical properties, in the negative-negative range, are such that the scattered intensity is minimum in the forward direction. In particular, μ=-4.55 for every particle size and ε=-1.06 (a=0.01λ), ε=-1.07 (a=0.02λ), ε=-1.09 (a=0.03λ), ε=-1.11 (a=0.04λ) and ε=-1.13 (a=0.05λ).

3.2.2 Distance effects on the directionality conditions: From far to near-field

Kerker's conditions, as have been remarked above, were deduced under the far-field approximation, that is ($2\pi r/\lambda >> 1$). If the observer tends to approach ($r/\lambda \leq 1$), directional effects on light scattering are affected. In a recent work (García-Cámara et al. 2010b), it has been shown that directional effects on light scattering of nanoparticles with optical properties under Kerker's conditions tends to disappear as r decreases. Figure 6 shows the scattered intensity measured on a line crossing a nanoparticle ($a \sim 0.01\lambda$) from the backward to the forward direction (Z-axis). Figure 6(a) is devoted to a particle satisfying the first Kerker's condition, while Figure 6(b) shows the same result when its relative optical constants fulfill the second Kerker's condition (eq. (22)). In both cases incident light is P-polarized (an orthogonal polarization produces similar results) and the case of a particle with the same value of ε and $\mu=1$ (non-directional case) is also plotted, for comparison purposes. For observation distances, $r > 0.16\lambda$, the directionality effects appears through a remarkable drop of the scattered intensity in either the backward (Figure 6a) or the forward direction (Figure 6b). However, as the observer approaches ($r \leq 0.16\lambda$), the evolution with the observation distance of the scattered intensity of a nanoparticle with directional features tends to that of a nanoparticle which optical constants do not satisfied any Kerker's condition.

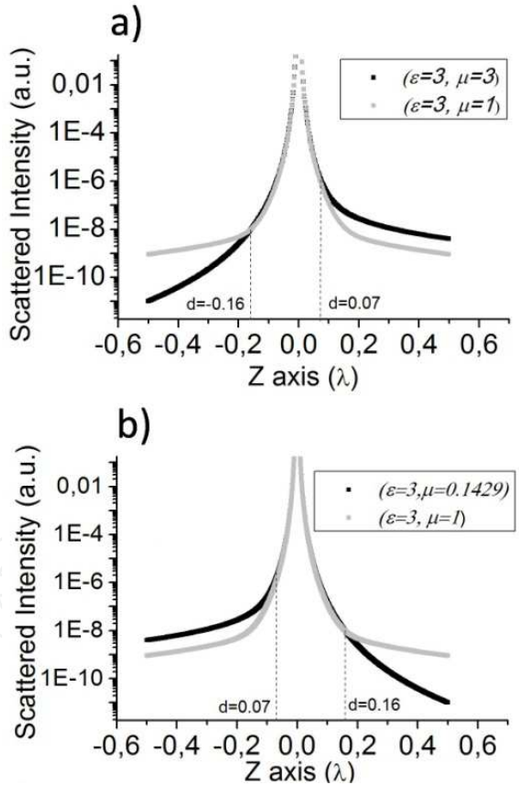

Fig. 6. Scattered intensity by a nanoparticle of radius $a=0.01\lambda$ and relative optical constants satisfying a) the first Kerker's condition ($\varepsilon=\mu=3$) or b) the second Kerker's condition ($\varepsilon=3$; $\mu=0.1429$) as a function of the distance from the particle surface in a direction parallel to the incident direction. For comparison, we have also included the case of a particle with ($\varepsilon=3$; $\mu=1$). In both cases the incident beam is polarized with the electric field parallel to the scattering plane.

3.3 A generalization of the Kerker's conditions

3.3.1 The zero-forward scattering condition and the optical theorem

In a recent research, Alù et al. (Alù & Engheta, 2011) stated that the *zero-forward scattering condition* (Eq. 22) is incongruent with the Optical Theorem. This relates the extinction efficiency (Q_{ext}) and the scattering amplitude in the forward direction [$S(0^o)$] as follows (Bohren & Huffman, 1983)

$$Q_{ext} = \frac{4}{x^2}\mathrm{Re}\{S(0^\circ)\} \tag{23}$$

When the *zero-forward scattering condition* holds, $S(0^o)=0$ and then $Q_{ext}=0$. This would imply that the particle would not scatter neither absorb electromagnetic radiation. However, in the examples shown in Figures 3 and 5, while the absorption is null because the optical constants are real, light scattering, and then the extinction efficiency, is non-zero at scattering angles other than $\theta=0^o$.

A first attempt to solve this apparent paradox is found in (Chylek & Pinnick, 1979) where they conclude that the dipolar approximation used by Kerker and co-workers is a non-unitary approximation because $Re(a_n) \geq |a_n|^2$, $Re(b_n) \geq |b_n|^2$ are not satisfied, and therefore the Optical Theorem cannot be applied. However, other more specific solutions to this paradox have been proposed recently. Alù et al (Alù & Engheta, 2011) established that, for a correct estimation of Q_{ext} it is crucial to include the radiative correction (Draine & Flatau, 1994) into the two first Mie coefficients (a_1 and b_1). From these considerations, energy conservation is warranted and, although the forward scattering is not zero, it is minimum with respect to other scattering angles. In addition, if the radiative correction is also included in the deduction of the *zero-forward scattering condition* (García-Cámara et al., 2011), a new condition can be found where both the Optical Theorem and the zero scattering at $\theta=0^o$ hold. This condition follows the equation

$$\varepsilon = \frac{\pi(4-\mu)-iVk^3(\mu-1)}{\pi(2\mu+1)-iVk^3(\mu-1)} \tag{24}$$

where V is the volume of the particle.

3.3.2 Directional effects at scattering angles other than forward and backward directions

Previous analysis on the distribution of the scattered intensity by a nanoparticle at both the forward and the backward direction can also be extended to other scattering angles. In a previous work (García-Cámara, 2010a), it is shown that by choosing a certain scattering angle different from 0^o and 180^o, there are pairs (ε; μ), which produce minimum scattered intensity within the scattering plane.

In Figure 7, we plot the scattering diagrams of a nanoparticle ($a = 0.01\lambda$) illuminated by a TE polarized incident beam. The optical constants are such that the scattered intensity is minimum at representative angles like 30^o, 60^o, 120^o and 150^o. Each diagram shows a double-

lobe structure with the position of the minimum depending on the particular values of the relative electric permittivity (ε) and the relative magnetic permeability (μ). Therefore, a suitable tuning of the material optical constants serves to control the angular position of the minimum of the scattered intensity.

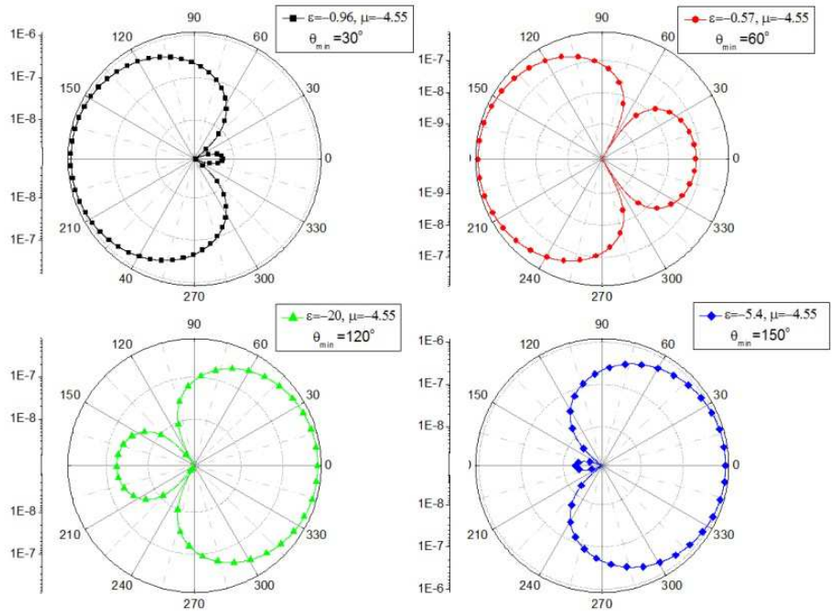

Fig. 7. Scattering diagrams of a spherical particle with $a = 0.01\lambda$ and relative optical constants in the negative-negative range (labeled in the figure) which produce a minimum scattering at certain scattering angles. The particle is illuminated with a linearly polarized incident plane wave with the electric field perpendicular to the scattering plane (TE polarization).

4. Directional effects on light scattering by dielectric particles

Previous analysis presented in this chapter about directional effects of light scattering have been done for nanoparticles with arbitrary values of both the relative electric permittivity (ε) and the relative magnetic permeability (μ) which do not correspond to any real material. In general, conventional materials do not show any stimulus to the magnetic field of electromagnetic radiation in the visible or the near-infrared region of the electromagnetic spectrum. For this reason, previous analyses have been considered an entelechy, as V. Veselago did in his work to generate and enrich scientific knowledge (Veselago, 1968). Very recently and looking for real situations, it has been shown that submicrometer particles made of Silicon (Evlyukhin et al, 2010 ; García-Extarri et al., 2011) or Germanium (Gómez-Medina et al, 2011b) present both effective electric and magnetic responses, corresponding to the dipolar contributions characterized by their first-order Mie coefficients, in the near-infrared range. Either of them can be selected by changing the illumination wavelength.

For this kind of nanoparticles, the spectral proximity of both dipolar electric and magnetic responses allows the appearance of coherent effects between dipolar modes. Consequently, under certain conditions, these scatterers are able to satisfy Kerker's conditions. Following the work made by Gómez-Medina et al. (Gómez-Medina et al, 2011b), in Figure 8, the

electric (α_e) and the magnetic (α_m) polarizabilities of a Ge nanoparticle of radius *a=240nm* are plotted as a function of the wavelength (λ) of the incident radiation. In the considered spectral range, Germanium has a refractive index which can be well approximated by a real constant *m=4 (*Palik, 1985*)*. Also the spectral evolution of the extinction efficiency (Q_{ext}) has been included in order to show the resonant behaviors that appear in a Ge nanoparticle. A dipolar electric (DE) mode arises at *λ=1823 nm,* while a dipolar magnetic (DM) resonance is located at *λ=2193 nm*. The vertical lines point the wavelengths at which either the first ($\alpha_e = \alpha_m$) or the second ($Re(\alpha_e)=-Re(\alpha_e)$ and $Im(\alpha_e)= Im(\alpha_e)$) Kerker's condition are fulfilled.

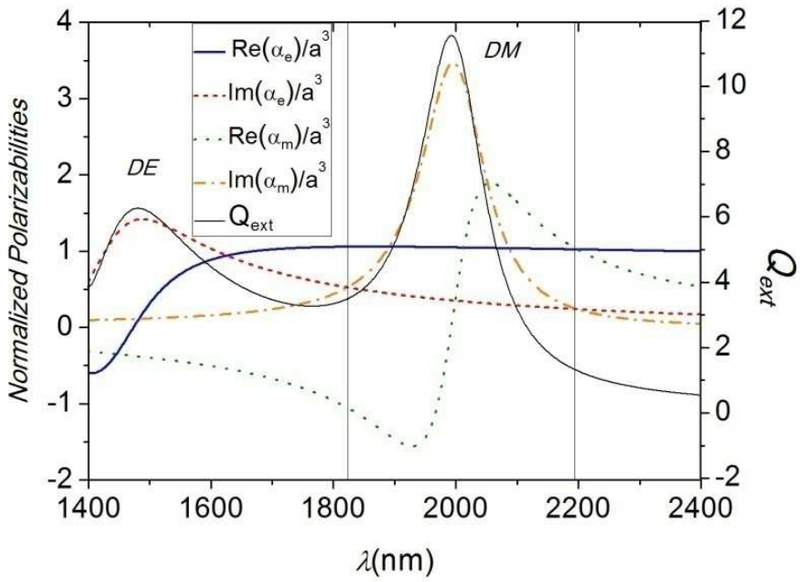

Fig. 8. Real and imaginary parts of the electric (α_e) and the magnetic (α_m) polarizabilities for a Ge nanoparticle (*a=240nm*). The refractive index of Germanium, in the considered range, can be considered as real and constant, *m≅4+0i.* The wavelengths at which the first and second Kerker's conditions (*λ=2193nm* and *λ=1823 nm*, respectively) are satisfied, are identified with vertical lines. Also, for comparison purposes, the extinction efficiency is plotted identifying the dipolar electric (DE) and the dipolar magnetic (DM) resonances.

The fact that a dielectric and non-magnetic particle (ε>0 and μ=1) presents both dipolar electric and also dipolar magnetic modes is quite interesting and could be useful for potential applications. For instance, this kind of resonances has been currently used for several tasks in a wide range of fields, ranging from the design of nanodevices (Maier et al, 2003; Anker et al., 2008) to biomedical treatments (Zemp, 2009). Unfortunately, they were observed only in metallic materials which present strong absorption losses. One of the advantages of dielectric materials, like Germanium or Silicon, is that they show negligible absorption in the considered range (Palik, 1985) and then losses are almost absent.

The position and shape of the dipolar resonances shown in Fig. 8 for Ge particles (similarly for Si particles) produces interesting coherent effects between them and consequently a natural way of reproducing Kerker's conditions by means of real materials. In order to verify that these directional features show up, Figure 9 plots the scattering diagrams of a Ge

nanosphere (*a=240nm*) when the incident wavelengths are those marked by vertical lines in Figure 8. The *zero-backward scattering condition* is satisfied for *λ=1823 nm,* and there is no scattered intensity in this direction (Figure 9a). However, the *zero-forward scattering condition* is strongly affected by size effects (Figure 9b). As was described in Section 3.2.1, the size of the particle prevents scattered intensity to be completely suppressed in the forward direction. However, its value is very small compared with those at other scattering angles and most part of the scattered intensity is located in the backward hemisphere ($\pi<\theta<2\pi$).

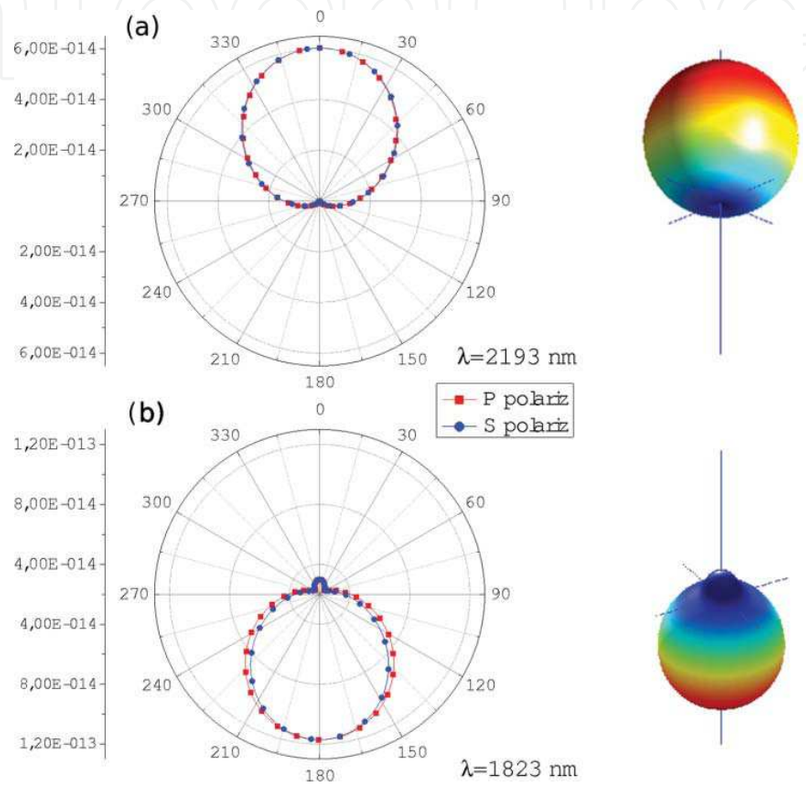

Fig. 9. Scattering diagrams for a Ge nanoparticles (*a=240nm*) illuminated by a linear polarized plane wave. Both polarizations, with the incident electric field parallel (TM or P polarization) or normal (TE or S polarization) to the scattering plane are considered. The incident wavelength is labeled in the figure. From (Gómez-Medina et al., 2011b).

Previous results for Germanium can also be extended to Silicon nanoparticles. These behaviors in Silicon could be even more interesting due to the wide range of applications of this material. Silicon is the base of microelectronics due to its semiconductor character and also to its abundance in Earth. For this reason, the industry of Silicon is very well developed. These new scattering features in the nanometric range could be the base for the development of new silicon applications as, for instance, optical nanocircuits.

5. Optical forces

Light carries energy and both linear and angular momenta that can be transferred to atoms, molecules and particles. Demonstration of levitation and trapping of micron-sized particles

by radiation pressure dates back to 1970 and the experiments reported by Ashkin and co-workers (Ashkin, 1970). Light forces on small particles are usually described as the sum of two terms: the dipole or gradient force and the radiation pressure or scattering force (Askhin et al., 1986; Neuman & Block, 2004; Novotny & Hecht, 2006; Chaumet & Nieto-Vesperinas 2000b; Gómez-Medina et al., 2001; Chaumet & Nieto-Vesperinas, 2002; Nieto-Vesperinas et al., 2004; Gómez-Medina & Saénz, 2004). There is an additional non-conservative curl force arising in a light field of non-uniform ellipticity that is proportional to the curl of the spin angular momentum of the light field (Albaladejo et al., 2009a; Nieto-Vesperinas et al., 2010). In analogy with electrostatics, small particles develop an electric (magnetic) dipole moment in response to the light electric (magnetic) field. The induced dipole is then drawn by field intensity gradients which compete with radiation pressure due to momentum transferred from the photons in the beam. By fashioning proper optical field gradients it is possible to trap and manipulate small dielectric particles with optical tweezers (Askhin et al, 1986; Neuman & Block, 2004) or create atomic arrays in optical lattices (Verkerk et al., 1992; Hemmerich & H'ansch, 1993). Intense optical fields can also induce significant forces between particles (Burns et al., 1989; Burns et al., 1990; Tartakova et al., 2002; Chaumet & Nieto-Vesperinas, 2001; Gómez-Medina & Saénz, 2004). Some previous work focused on optical forces on macroscopic media, either with electric (Mansuripur, 2004) or magnetic response (Kemp et al., 2005; Mansuripur, 2007), or particles with electric response (Kemp et al., 2006a). Radiation pressure forces on dielectric and magnetic particles under plane wave incidence have been computed for both small cylinders (Kemp et al., 2006b) and spheres (Lakhtakia & Mulholland, 1993; Lakhtakia, 2008). The total force on an electric and magnetic dipolar particle has been shown (Chaumet & Rahmani, 2009; Nieto-Vesperinas et al., 2010; Nieto-Vesperinas et al., 2011; Gómez-Medina et al., 2011a; Gómez-Medina et al., 2011b) to have a similarity with that previously obtained for electric dipoles. Moreover, in the presence of both electric and magnetic responses, the force presents an additional term proportional to the cross product of the electric and magnetic dipoles (Chaumet & Rahmani, 2009; Nieto-Vesperinas et al., 2010; Nieto-Vesperinas et al., 2011; Gómez-Medina et al., 2011a; Gómez-Medina et al., 2011b). The relevance and physical origin of this electric-magnetic dipolar interaction term for a single particle has been recently discussed (Nieto-Vesperinas et al., 2010; Nieto-Vesperinas et al., 2011; Gómez-Medina et al., 2011a; Gómez-Medina et al., 2011b)

5.1 Force on a small particle with electric and magnetic response to an electromagnetic wave

We consider a dipolar particle embedded in a non-dissipative medium with relative dielectric permittivity ε and magnetic permeability μ, subjected to an incident electromagnetic field whose electric and magnetic vectors are $\boldsymbol{E}^{(i)}$ and $\boldsymbol{B}^{(i)}$, respectively. The total time-averaged electromagnetic force acting on the particle is (Chaumet & Nieto-Vesperinas, 2000; Jackson, 1998; Nieto-Vesperinas et al., 2010):

$$\langle \mathbf{F} \rangle = \frac{1}{8\pi} \Re \left\{ \int_S \left[\varepsilon (\mathbf{E} \cdot \mathbf{s}) \mathbf{E}^* + \mu^{-1} (\mathbf{B} \cdot \mathbf{s}) \mathbf{B}^* - \frac{1}{2} \left(\varepsilon |\mathbf{E}|^2 + \mu^{-1} |\mathbf{B}|^{-1} \right) \mathbf{s} \right] dS \right\}, \tag{25}$$

where $\Re$ stands for real part, dS denotes the element of any surface S that encloses the particle.

The fields in Eq. (25) are total fields, namely the sum of the incident and scattered (re-radiated) fields: $\boldsymbol{E}^{(i)}+\boldsymbol{E}^{(r)}$, $\boldsymbol{B}^{(i)}+\boldsymbol{B}^{(r)}$. $\mathbf{s}$ is its local outward unit normal. A time dependence $e^{(-iwt)}$ is assumed throughout. For a small particle, within the range of validity of the dipolar approximation, the scattered field corresponds to that radiated by the induced electric and magnetic dipole moments, $\boldsymbol{p}$ and $\boldsymbol{m}$, respectively. In this case, Eq. (25) leads to the expression

$$\langle \mathbf{F} \rangle = \frac{1}{2}\Re\left\{ \mathbf{p}\left(\nabla \otimes \mathbf{E}^{(i)*}\right) + \mathbf{m}\left(\nabla \otimes \mathbf{B}^{(i)*}\right) - \frac{2k^4}{3}\sqrt{\frac{\mu}{\varepsilon}}\left(\mathbf{p}\times\mathbf{m}^*\right)\right\} \tag{26}$$

Equation (26) represents the generalization of the result of (Chaumet & Rahmani, 2009) for the time-averaged force on a particle immersed in an arbitrary medium with refractive index: $m=\sqrt{\varepsilon\mu}$. The wavenumber is $k = m\omega/c$, ω being the frequency. The symbol $\otimes$ represents the dyadic product so that the matrix operation: $\mathbf{W}(\nabla \otimes \mathbf{V})$ has elements $W_j\partial_j V_j$ for $i, j = 1, 2\ 3$. All variables in Eq. (26) are evaluated at a point $\boldsymbol{r} = \boldsymbol{r}_0$ in the particle. The first term of Eq. (26) is the force $< \mathbf{F}_e >$ exerted by the incident field on the induced electric dipole, the second and third terms $< \mathbf{F}_m >$ and $< \mathbf{F}_{em} >$ are the force on the induced magnetic dipole and the force due to the interaction between both dipoles (Chaumet & Rahmani, 2009; Nieto-Vesperinas et al., 2010).

5.2 Optical theorem and forces on an electric and magnetic dipolar particle

The question of energy conservation has been recurrently addressed and debated as regards small particles (Chýlek & Pinnick, 1979; Lock et al., 1995), especially in connection with magnetic particles that produce zero-forward scattering intensity (Alù & Engheta, 2011; Nieto-Vesperinas et al., 2011; García-Cámara et al., 2011; Gómez-Medina et al., 2011b). It is thus relevant to explore the formal analogy between the force as momentum "absorption" rate and the optical theorem expressing the conservation of electromagnetic energy. From the Poynting's theorem (Bohren & Huffman, 1983; Jackson, 1998), the rate $-W^{(a)}$ at which energy is being absorbed by the particle is given by

$$-W^{(a)} = \int_S \left\{ \langle \mathbf{S} \rangle - \left\langle \mathbf{S}^{(i)} \right\rangle \right\} \mathbf{s}\, dS \tag{27}$$

$$= \frac{c}{8\pi m}\Re\left\{ \int_S \varepsilon(\mathbf{E}\cdot\mathbf{s})\mathbf{E}^* + \mu^{-1}(\mathbf{B}\cdot\mathbf{s})\mathbf{B}^* - \frac{1}{2}\left(\varepsilon|\mathbf{E}|^2 + \mu^{-1}|\mathbf{B}|^{-1}\right) dS \right\} \tag{28}$$

By introducing the incident field as a decomposition of plane wave components and taking the sphere S in Eq. (27) so large that $k|r-r_0|\to\infty$, and using Jones' lemma based on the principle of the stationary phase, (see Appendix XII of Bohren & Huffman, 1983), and the source-free condition, we get the optical theorem for an arbitrary field (Nieto-Vesperinas et al., 2010):

$$-W^{(a)} = -\frac{\omega}{2}\Im\left\{ \mathbf{p}\cdot\mathbf{E}^{(i)*}(r_0)\right\} - \frac{\omega}{2}\Im\left\{ \mathbf{m}\cdot\mathbf{B}^{(i)}(r_0)\right\} + \frac{c}{m}\frac{k^4}{3}\left(\varepsilon^{-1}|\mathbf{p}|^2 + \mu|\mathbf{m}|^2\right). \tag{29}$$

The first two terms of Eq. (29), coming from the interference between the incident and radiated fields, are the energy analogue of the electric and magnetic dipolar forces given by first two terms in Eq. (26).

The third and fourth terms of Eq. (29) that come from the integral of the third and fourth terms of Eq. (28), now yield the rate $W^{(s)}$ at which the energy is being scattered, which together with the left hand side of this equation contributes to the rate of energy extinction by the particle $W^{(a)}+W^{(s)}$:

$$W^{(a)}+W^{(s)}=\frac{\omega}{2}\Im\left\{\mathbf{p}\cdot\mathbf{E}^{(i)*}(r_0)\right\}+\frac{\omega}{2}\Im\left\{\mathbf{m}\cdot\mathbf{B}^{(i)*}(r_0)\right\}. \tag{30}$$

Analogously as with the rate of scattered energy, the electric-magnetic dipolar interaction term of the force (third term of Eq. (26)) corresponds to the rate at which momentum is being scattered by the particle. We shall explore in some detail this analogy in order to illustrate the physical origin of $<\mathbf{F}_{em}>$. We notice that the power density of the scattered field can be written as the sum of two terms (Nieto-Vesperinas et al., 2010)

$$\left\langle\mathbf{S}^{(r)}\right\rangle dS=\frac{c}{8\pi m}k^4\left(\varepsilon^{-1}\left|\mathbf{p}\times\mathbf{s}\right|^2+\mu\left|\mathbf{m}\times\mathbf{s}\right|^2\right)s\,d\Omega$$

$$+\frac{c}{4\pi m}k^4\sqrt{\frac{\mu}{\varepsilon}}\Re\left\{(\mathbf{s}\times\mathbf{p})\cdot\mathbf{m}^*\right\}\mathbf{s}\,d\Omega\,. \tag{31}$$

where the second term of Eq. (31) corresponds to the interference between the electric and magnetic dipolar fields. After integration over the closed surface S, that second term does not contribute to the radiated power, while it is the only contribution to the electric-magnetic dipolar interaction term of the force in Eq. (26). Namely, $<\mathbf{F}_{em}>$ comes from the interference between the fields radiated by **p** and **m**.

5.3 Forces on an electric and magnetic dipolar particle for plane wave incidence

In order to illustrate the relevance of the different terms in the optical forces, we shall next consider the force from a plane wave $E^{(i)}=e^{(i)}e^{iks_0\cdot r}$, $B^{(i)}=b^{(i)}e^{iks_0\cdot r}$ with $\mathbf{e}^{(i)}=\left\{\mathbf{b}^{(i)}\times\mathbf{s}_0\right\}/m$ on a small dielectric and magnetic spherical particle characterized by its electric and magnetic polarizabilities α_e and α_m. When the induced dipole moments are expressed in terms of the incident field, i.e.

$$\mathbf{p}=\alpha_e\mathbf{e}^{(i)};\quad\mathbf{m}=\alpha_m\mathbf{b}^{(i)}. \tag{32}$$

For plane wave incidence, the total force is given by (Nieto-Vesperinas et al., 2010):

$$\langle\mathbf{F}\rangle\;=\;\langle\mathbf{F}_e\rangle+\langle\mathbf{F}_m\rangle+\langle\mathbf{F}_{em}\rangle$$

$$=\mathrm{s}_0\frac{k}{2}\Im\left\{\mathbf{p}\cdot\mathbf{e}^{(i)*}+\mathbf{m}\cdot\mathbf{b}^{(i)*}\right\}-\frac{\mathrm{m}}{\mathrm{c}}\int_S\left\langle\mathbf{S}^{(r)}\right\rangle dS \tag{33}$$

$$= s_0 F_0 \left[\Im\left\{\varepsilon^{-1}\alpha_e\right\} + \Im\{\mu\alpha_m\} - \frac{2k^3}{3}\frac{\mu}{\varepsilon}\Re\left\{\alpha_e \alpha_m^{*}\right\} \right], \tag{34}$$

where $F_0 = \varepsilon \left|\mathbf{e}^{(i)}\right|^2 / 2$. The first two terms, $< \mathbf{F}_e >$ and $< \mathbf{F}_m >$, correspond to the forces on to the sum of radiation pressures for a pure electric and a pure magnetic dipole, respectively. The third term, $< \mathbf{F}_{em} >$, is the time-averaged scattered momentum rate, and we shall see below that it also contributes to radiation pressure (Nieto-Vesperinas et al., 2010; Gómez-Medina et al., 2011a) and it is related to the asymmetry in the scattered intensity distribution (Nieto-Vesperinas et al., 2011; Gómez-Medina et al., 2011b).

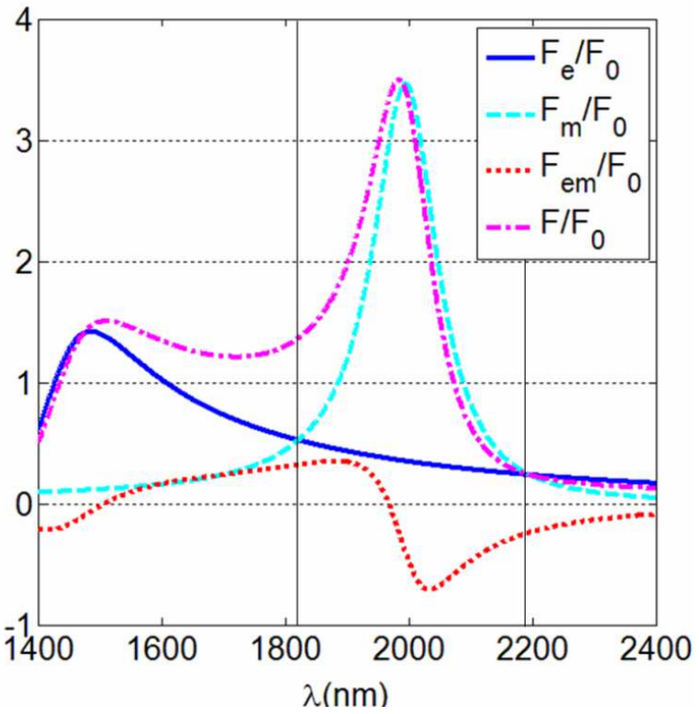

Fig. 10. Different contributions to the total radiation pressure versus the wavelength, for the Ge particle of Figs. 8-9. Normalization is done by $F_0 = \varepsilon \left|\mathbf{e}^{(i)}\right|^2 / 2$. The vertical lines mark the first and second generalized Kerker's conditions. Notice that when the first generalized Kerker's condition is fulfilled, i.e., $\Re\{\alpha_e\} = \Re\{\alpha_m\}$ and $\Im\{\alpha_e\} = \Im\{\alpha_m\}$, $\langle \mathbf{F} \rangle = \langle \mathbf{F}_e \rangle = \langle \mathbf{F}_m \rangle = -\langle \mathbf{F}_{em} \rangle$. From (Gómez-Medina et al. 2011b).

5.4 The generalized Kerker's conditions on optical forces

From Eqs. (6) and (34), one derives for the radiation pressure force (Nieto-Vesperinas et al., 2011):

$$\langle \mathbf{F} \rangle = s_0 F_0 \frac{1}{6k}\left[\frac{dC_{sca}}{d\Omega}\left(0^{\circ}\right) + 3\frac{dC_{sca}}{d\Omega}\left(180^{\circ}\right) - \frac{3}{2\pi}C_{abs} \right]. \tag{35}$$

Equation (35) emphasizes the dominant role of the backward scattering on radiation pressure forces.

At the first generalized Kerker's condition, the interference term of Eqs. (34-35) cancels out the magnetic contribution and we obtain $< \mathbf{F} > = < \mathbf{F}_e >$. At the second generalized Kerker's condition, where the backscattering is enhanced, $< \mathbf{F} > = 3< \mathbf{F}_e >$. Notice that at both generalized Kerker's conditions the scattering cross section is exactly the same; however, the radiation pressures differ by a factor of 3. These properties are illustrated in Figure 10, where we show the different contributions to the total time averaged force on a submicrometer Ge particle.

The strong peak in the radiation pressure force is mainly dominated by the first "magnetic" Mie resonance. This is striking and in contrast with all previous beliefs about optical forces on dipolar dielectric particles, that assumed that these forces would solely be described by the electric polarizability. It is also common to assume that for dielectric particles the real part of the polarizability is much larger than its imaginary part. As a matter of fact, this is behind the development of optical tweezers, in which gradient forces (that are proportional to $\Re(\alpha_e)$), dominate over the radiation pressure or scattering force contribution (which is proportional to $\Im(\alpha_e)$) (Volpe et al., 2006). However, as the size of the particle increases, and for any dielectric particle, there is a crossover from electric to magnetic response as we approach the first Mie resonance, the point at which the response is absolutely dominated by the magnetic dipole. Moreover, just at the resonance, and in absence of absorption, $\Re(\alpha_m)=0$ and $\Im(\alpha_m)=3/(\mu 2k^3)$. Then, the radiation pressure contribution of the magnetic term dominates the total force $\langle \mathbf{F} \rangle \cong \langle \mathbf{F}_m \rangle \approx \mathbf{S}_0 \left(\varepsilon \left| \mathbf{e}^{(i)} \right|^2 / 2 \right) \left[3/2k^3 \right]$. Namely, in resonance the radiation pressure force presents a strong peak, the maximum force being independent of both material parameters and particle radius.

6. Conclusion

In this chapter we have analyzed the main aspects of one of the most interesting phenomena of light scattering by nanoparticles: the possibility to control its angular distribution (directionality). As it has been shown, a general magneto-dielectric particle, with suitable values of its relative optical constants (ε, μ), could present directional effects resulting from a coherent effect between real and imaginary parts of both electric and magnetic polarizabilities. The control of this effect could improve the characteristics of many current applications which employ nanoparticles. Also, it can be the base of new potential applications related with light guidance in low dimensions, as for instance, intra- or inter-chip optical communications (García-Cámara; 2011b). In addition, we showed that these scattering effects also affect the radiation pressure on these small particles. Thus, the "non-usual" scattering properties discussed before will strongly affect the dynamics of particle confinement in optical traps and vortex lattices (Albaladejo et al., 2009b; Gómez-Medina et al., 2011a; Albaladejo et al., 2011) governed by both gradient and curl forces.

Finally, we have showed that small dielectric particles made of non magnetic materials present scattering properties similar to those previously reported for hypothetical magneto-dielectric particles. In particular, it has been shown that submicrometer Germanium particles present these directional phenomena in light scattering in the near-infrared range. These studies could serve as a stimulus for new experiments which implement these non-conventional phenomena.

7. Acknowledgment

This work has been supported by the EU NMP3-SL-2008-214107-Nanomagma, the Spanish MICINN Consolider NanoLight (CSD2007-00046), FIS2010-21984, FIS2009-13430-C01-C02, and FIS2007-60158, as well as by the Comunidad de Madrid Microseres-CM (S2009/TIC-1476). B.G.-C. wants to express his gratitude to the University of Cantabria for his postdoctoral fellowship. Work by R.G.-M. was supported by the MICINN "Juan de la Cierva" Fellowship.

8. References

Albaladejo, S.; Marqués, M.I.; Laroche, M. & Sáenz, J.J. (2009). Scattering forces from the curl of the spin angular momentum of a light field. *Physical Review Letters* Vol. 102, No. 11 (March 2009), pp. 113602, ISNN 0031-9007.

Albaladejo, S.; Marqués, M.I. & Sáenz, J.J. (2011). Light control of silver nanoparticle's diffusion. *NanoLetters*, Vol. 9, No. 10 (October 2009), pp. 3527-3531, ISNN 1530-6984.

Albaladejo, S.; Marqués, M.I. & Sáenz, J.J. (2011). Light control of silver nanoparticle's diffusion. *Optics Express*, Vol. 19, No. 12 (June 2011), pp. 11471-11478, ISNN 1094-4087.

Alù, A. & Engheta, N. (2011). How does forward-scattering in magnetodielectric nanoparticles comply with the optical theorem? *Journal of Nanophotonics*, Vol. 4 (May 2010), pp. 041590, ISSN 1934-2608.

Anker, J.N.; Hall, W.P.; Lyandres, O.; Shan, N. C.; Zhao, J. & Van Duyne, R.P. (2008) Biosensing with plasmonic nanosensors. *Nature Materials,* Vol. 7, No. 6, pp. 442-453, ISSN 1476-1122.

Ashkin, A. (1970). Acceleration and Trapping of Particles by Radiation Pressure. *Physical Review Letters,* Vol. 24, No. 4 (January 1970), pp. 156–159, ISNN 1079-7114.

Ashkin, A.; Dziedzic, J. M.; Bjorkholm, J. E. & Chu, S. (1986). Observation of a single-beam gradient force optical trap for dielectric particles. *Optics Letters, Vol.* 11, No. 5 (May 1986), pp. 288–290, ISNN 0146-9592.

Bohren, C.F & Huffman, D.R. (Eds.). (1983). *Absorption and Scattering of Light by Small Particles,* John Wiley& Sons, ISBN 0-471-05772-X, New York.

Burns, M.M.; Fournier, J.M. & Golovchenko, J.A. (1989). Optical Binding. *Physical Review Letters,* Vol. 63, No. 12 (September 1989), pp. 1233–1236, ISNN 1079-7114.

Burns, M.M.; Fournier, J.M. & Golovchenko, J.A. (1990). Optical Matter: Crystallization and Binding in Intense Optical Fields. *Science*, Vol. 249, No. 4970 (August 1990), pp. 749–754, ISNN 0036-8075.

Chaumet, P.C. & Nieto-Vesperinas, M. (2000). Coupled dipole method determination of the electromagnetic force on a particle over a flat dielectric substrate. *Physical Review B,* Vol. 61, No. 20 (May 2000), pp. 14119–14127, ISNN 1098-0121.

Chaumet, P.C. & Nieto-Vesperinas, M. (2000). Electromagnetic force on a metallic particle in the presence of a dielectric surface. *Physical Review B,* Vol. 62, No. 16 (October 2000), pp. 11185–11191, ISNN 1098-0121.

Chaumet, P.C. & Nieto-Vesperinas, M. (2001). Optical binding of particles with or without the presence of a flat dielectric surface. *Physical Review B*, Vol. 64, No. 3 (June 2001), pp. 035422–0354227, ISNN 1098-0121.

Chaumet, P.C.; Rahmani, A. and & Nieto-Vesperinas, M. (2002). Optical trapping and manipulation of nano-objects with an apertureless probe. *Physical Review Letters*, Vol. 88, No. 12 (March 2002), pp. 123601-123604, ISNN 1079-7114.

Chaumet, P.C. & Rahmani, A. (2009). Electromagnetic force and torque on magnetic and negative-index scatterers. *Optics Express,* Vol. 17, No. 4 (February 2009), pp. 2224–2234, ISNN 1094-4087.

Chýlek, P. & Pinnick, R.G. (1979). Nonunitarity of light scattering approximations. *Applied Optics*, Vol. 18, No. 8 (April, 1979), pp.1123-1124, ISSN 1559-128X.

Draine, B.T. & Flatau, P.J. (1994). Discrete-dipole approximation for scattering calculations. *Journal of the Optical Society of America A*, Vol. 11, No. 4 (April 1994), pp. 1491-1499, ISSN 1084-7529.

Evlyyukhin, A.B.; Reinhardt, C.; Seidel, A.; Luk'yanchuk, B.S. & Chichkov, B.N. (2010). Optical response features of Si-nanoparticle arrays. *Physical Review B,* Vol. 82, No. 4 (July 2010), pp. 045404, ISSN 1098-0121.

Gao, H.; Hyun, J.K.; Lee, M.H.; Yang, J.-C.; Lauhon, L.J. & Odom, T.W. (2010). Broadband plasmonic microlenses based on patches of nanoholes. *Nano Letters*, Vol 10. No. 10 (September 2010), pp. 4111-4116, ISSN 1530-6984.

García-Cámara, B.; Saiz, J.M.; González, F. & Moreno, F. (2010). Nanoparticles with unconventional properties: Size effects. *Optics Communications*, Vol. 283, No. 3 (February, 2010), pp. 490-496, ISNN 0030-4018.

García-Cámara B.; Saiz, J.M.; González, F. & Moreno, F. (2010). Distance limit of the directionality conditions for the scattering of nanoparticles. *Metamaterials,* Vol. 4, No. 1 (May 2010), pp. 15-23, ISSN 1873-1988.

García-Cámara, B.; Alcaraz de la Osa, R.; Saiz, J.M.; González, F. & Moreno, F. (2011). Directionality in scattering by nanoparticles: Kerker's null-scattering conditions revisited. *Optics Letters,* Vol. 36, No. 5 (February, 2011), pp. 728-730, ISSN 0146-9592.

García-Cámara, B. (2011), Inta-/Inter-chip optical communications: High speed and low dimensions, In: *Communication architecture for systems-on-chip*, J.L. Ayala (Ed.), pp. 249-322, CRC Press, ISBN 978-1-4398-4170-9, Florida (USA).

García-Etxarri, A.; Gómez-Medina, R.; Froufe-Pérez, L.S.; López, C.; Chantada, L.; Scheffold F.; Aizpurua, J.; Nieto-Vesperinas, M. & Sáenz, J.J. (2011). Strong magnetic response of submicrometer silicon particles in the infrared. *Optics Express,* Vol. 19, No. 6 (February, 2011), pp. 4815-4826, ISSN 1094-4087.

Gómez-Medina, R.; San José, P.; García-Martín, A.; Lester, M.; Nieto-Vesperinas, M. & Sáenz, J.J. (2001). Resonant radiation pressure on neutral particles in a waveguide *Physical Review Letters*, Vol. 86, No. 19 (May 2001), pp. 4275-4277, ISNN 1079-7114.

Gómez-Medina, R. & Saénz J.J. (2004). Unusually Strong Optical Interactions between Particles in Quasi-One-Dimensional Geometries. *Physical Review Letters*, Vol. 93, No. 24 (December 2004), pp. 243602–243605, ISNN 1079-7114.

Gómez-Medina, R.; Nieto-Vesperinas, M. & Saénz J.J. (2011). Nonconservative electric and magnetic optical forces on submicrometer dielectric particles. *Physical Review A*, Vol. 83, No. 3 (March 2011), pp. 033825, ISSN 1050-2947.

Gómez-Medina, R.; García-Cámara, B.; Suárez-Lacalle, I.; González, F.; Moreno, F.; Nieto-Vesperinas, M. & Saénz J.J. (2011). Electric and Magnetic dipolar response of

germanium nanospheres: interference effects, scattering anisotropy, and optical forces. *Journal of Nanophotonics* , Vol. 5 (June, 2011), pp. 053512, ISSN 1934-2608.

Hemmerich A. & H¨ansch, T.W. (1993). Two-dimesional atomic crystal bound by light. *Physical Review Letters*, Vol. 70, No. 4 (January 1993), pp. 410–413, ISNN 1079-7114.

Jackson, J.D. (1998). *Classical Electrodynamics*, 3rd edition, John Wiley, New York.

Jessen, P.S.; Gerz, C.; Lett, P.D.; Phillips, W.D.; Rolston, S.L.; Spreeuw, R.J.C. & Westbrook, C.I. (1992). Observation of quantized motion of Rb atoms in an optical field. *Physical Review Letters*, Vol. 69, No. 1 (July 1992), pp. 49–52, ISNN 1079-7114.

Kemp, B.A.; Grzegorczyk, T.M. & Kong, J.A. (2005). Ab initio study of the radiation pressure on dielectric and magnetic media. *Optics Express*, Vol. 13, No. 23 (November 2005) pp. 9280-9291, eISNN 1094-4087.

Kemp, B.A.; Grzegorczyk, T.M. & Kong, J.A. (2006). Optical momentum transfer to absorbing Mie particles. *Physical Review Letters,* Vol. 97, No. 13 (September 2006), pp. 133902, ISNN 1079-7114.

Kemp, B.A.; Grzegorczyk, T.M. & Kong, J.A. (2006). Lorentz force on dielectric and magnetic particles. *Journal of Electromagnetics Waves and Applications,* Vol. 20, No. 6 (June 2006), pp. 827–839, ISNN 0920-5071.

Kerker, M.; Wang, D. & Giles G. (1983). Electromagnetic scattering by magnetic spheres. *Journal of the Optical Society of America*, Vol. 73, No. 6 (June, 1983), pp. 756-767, ISSN 0030-3941.

Lakhtakia, A. (2008) Radiation pressure efficiencies of spheres made of isotropic, achiral, passive, homogeneous, negative-phase-velocity materials. *Electromagnetics,* Vol. 28, No. 5 (June 2008), pp. 346–353, ISNN 0272-6343.

Lakhtakia A. & Mulholland, G.W. (1993). On two numerical techniques for light scattering by dielectric agglomerated structures. Journal of Research of the National Institute of Standards and Technology, Vol. 98, No. 6 (December 1993), pp. 699–716, ISNN 1044-677X.

Lock, J. A.; Hodges, J.T. & Gouesbet, G. (1995) Failure of the optical theorem for Gaussian-beam scattering by a spherical particle. *Journal of the Optical Society of America A,* Vol. 12, No. 12 (December 1995), pp. 2708–2715, ISSN 1084-7529.

Maier, S. A.; Kik, P. G.; Atwater, H. A.; Meltzer, S.; Harel, E.; Koel B. E. & Requicha, A. G. (2003). Local detection of electromagnetic energy transport below the diffraction limit in metal nanoparticle Plasmon waveguides. *Nature Materials*, Vol. 2, No. 4 (April 2003), pp. 229-232, ISSN 1476-1122.

Mansuripur, M. (2004). Radiation pressure and the linear momentum of the electromagnetic field. *Optics Express,* Vol.12, No 22 (November 2004). pp. 5375–5401, eISNN 1094-4087.

Mansuripur, M. (2007). Radiation pressure and the linear momentum of the electromagnetic field in magnetic media. *Optics Express*, Vol. 15, No.21 (October 2007), pp. 13502-13518, eISNN 1094-4087.

Mirin, N. A. & Halas, N. J. (2009).Light-bending nanoparticles. *Nano Letters*, Vol 9, No. 3 (February 2009), pp. 1255-1259, ISSN 1530-6984.

Neuman, K. C. & Block, S. M. (2004). Optical trapping. *Review of Scientific Instruments*, Vol. 75, No. 9 (September 2004), pp. 2787–2809, ISSN 0034-6748.

Nieto-Vesperinas, M. & García, N. Comment on "Negative refraction makes a perfect lens". *Physical Review Letters*, Vol. 91, No. 9 (August 2003), pp. 099702, ISSN 1079-7114.

Nieto-Vesperinas, M.; Chaumet, P.C. & Rahmani, A. (2004). Near field photonic forces. *Philosophical Transactions of the Royal Society of London A,* Vol. 362, No. 1817 (February 2004), pp. 719–737, ISSN 1471-2962.

Nieto-Vesperinas, M.; Sáenz, J.J.; Gómez-Medina, R.; & Chantada, L. (2010). Optical forces on small magnetodielectric particles. *Optics Express,* Vol. 18, No. 11 (May 2010), pp. 11428–11443, eISNN 1094-4087.

Nieto-Vesperinas, M.; Gómez-Medina, R. & Sáenz, J.J. (2011). Angle-suppressed scattering and optical forces on submicrometer dielectric particles. *Journal of the Optical Society of America A,* Vol. 28, No. 1 (December 2010), pp. 54–60, ISSN 1084-7529.

Novotny, L. & Hecht, B. (2006). *Principles of Nano-Optics*. Cambridge University Press, Cambridge.

Palik, E.D. (Ed.). (1985), *Handbook of Optical Constants of Solids,* Academis Press, ISBN 0-12-544420-6 , Orlando, Florida

Pendry, J.B.; Schuring D. & Smith D.R. (2006). Controlling electromagnetic fields. *Science*, Vol. 312, N0. 5781 (June 2006), pp. 1780-1782, ISSN 0036-8075.

Pendry, J.B. (2000). Negative refraction makes perfect lens. *Physical Review Letters*, Vol. 85. No. 18 (October 2000), pp. 3966-3969, ISNN 1079-7114.

Prasad, P. N. (2004). *Nanophotonics,* John Wiley& Sons, ISBN 0471649880, New York.

Shalaev, V.M. (2008). Transforming light. *Science*, Vol. 322, No. 5900 (October 2008), pp. 384-386, ISSN 0036-8075.

Tatarkova, S.A.; Carruthers, A.E. & Dholakia, K. (2002). One-Dimensional Optically Bound Arrays of Microscopic Particles. *Physical Review Letters,* Vol. 89, No. 28 (December 2002), pp. 283901–283904, ISNN 1079-7114.

Verkerk, P.; Lounis, B.; Salomon, C.; Cohen-Tannoudji, C.; Courtois, J.-Y. & Grynberg, G. (1992). Dynamics and spatial order of cold cesium atoms in a periodic optical potential. *Physical Review Letters,* Vol. 68, No. 26 (June 1992), pp. 3861–3864, ISNN 1079-7114.

Veselago, V. (1968). The electrodynamics of substances with simultaneously negative values of ε and μ. *Soviet Physics Uspekhi*, Vol. 10, No. 4 (January 1968), pp. 509-514, ISNN 0038-5670.

Volpe, G. ; Quidant, R.; Badenes, G. & Petrov, D. (2006). Surface plasmon radiation forces. *Physical Review Letters*, Vol. 96, No. 23 (June 2006), pp. 238101, ISNN 1079-7114.

Zemp, R. J. (2009) Nanomedicine:Detecting rare cancer cells. *Nature Nanotechnology*, Vol. 4, No. 12 (December 2009), pp. 798-799, ISNN 1748-3387.

Zhedulev, N.I. (2010). The road ahead of metamaterials. *Science*, Vol. 328, No. 5978 (April, 2010), pp. 582-583, ISNN 0036-8075.

Zhu, J.; Ozdemir, S. K.; Xiao, Y.-F.; Li, L.; He, L.; Chen, D.- R. & Yang L. (2010). On-chip single nanoparticle detection and sizing by mode splitting in an ultrahigh-Q microresonator. *Nature Photonics*, Vol. 4, No. 1 (January, 2010), pp. 46-49, ISSN 1749-4885.

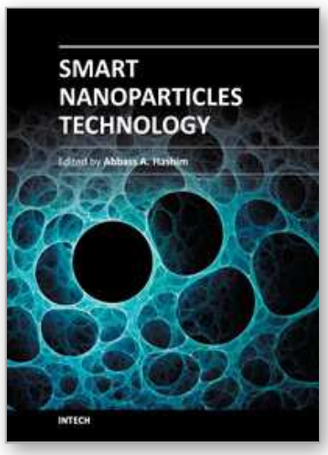

Smart Nanoparticles Technology

Edited by Dr. Abbass Hashim

ISBN 978-953-51-0500-8
Hard cover, 576 pages
Publisher InTech
Published online 18, April, 2012
Published in print edition April, 2012

In the last few years, Nanoparticles and their applications dramatically diverted science in the direction of brand new philosophy. The properties of many conventional materials changed when formed from nanoparticles. Nanoparticles have a greater surface area per weight than larger particles which causes them to be more reactive and effective than other molecules. In this book, we (InTech publisher, editor and authors) have invested a lot of effort to include 25 most advanced technology chapters. The book is organised into three well-heeled parts. We would like to invite all Nanotechnology scientists to read and share the knowledge and contents of this book.

How to reference

In order to correctly reference this scholarly work, feel free to copy and paste the following:

Braulio Garcia-Camara, Francisco Gonzalez, Fernando Moreno, Raquel Gomez-Medina, Juan Jose Saenz and Manuel Nieto-Vesperinas (2012). On the Optical Response of Nanoparticles: Directionality Effects and Optical Forces, Smart Nanoparticles Technology, Dr. Abbass Hashim (Ed.), ISBN: 978-953-51-0500-8, InTech, Available from: http://www.intechopen.com/books/smart-nanoparticles-technology/on-the-optical-response-of-nanoparticles-directionality-effects-and-optical-forces-

INTECH
open science | open minds

InTech Europe
University Campus STeP Ri
Slavka Krautzeka 83/A
51000 Rijeka, Croatia
Phone: +385 (51) 770 447
Fax: +385 (51) 686 166
www.intechopen.com

InTech China
Unit 405, Office Block, Hotel Equatorial Shanghai
No.65, Yan An Road (West), Shanghai, 200040, China
中国上海市延安西路65号上海国际贵都大饭店办公楼405单元
Phone: +86-21-62489820
Fax: +86-21-62489821

IntechOpen